Report of the CNR-STM: "Aerosol and cloud radiative effect evaluation in the frame of Interact II measurement campaign" by Simone Lolli

1. Introduction

According to the International Panel for Climate Change, (IPPC, 2014) one of the major uncertainties related to climate studies are the direct and indirect effects of the anthropogenic and natural aerosols and their interaction with meteorological phenomena. More in detail, the more recent estimation of the net aerosol radiative forcing are still affected by large uncertainties and its sign (indicating cooling or heating of the atmosphere) may easily switch between positive and negative or vice-versa. Clouds, especially thin cirrus clouds, represent another fundamental contribution to the Earth's radiative budget (Campbell et al., 2016). Their contribution is a feedback, both positive and negative, that is depending on their optical depth and altitude, which in turn is related to the temperature variations (influenced by aerosol direct effects). Due to this degree of complexity, an accurate evaluation of the vertically resolved cloud and aerosol optical properties it is of fundamental importance in order to improve the estimation of their impact on the radiation budget and to assess their mutual interactions (the direct/indirect effects) at global scale. The optical cloud and aerosol optical and microphysical properties are studied since decades using passive ground-based measurements (AERONET, Holben et al., 1998) or using satellite sensors (MODIS, MISR). Nevertheless, these measurements are not able to provide range-resolved atmospheric properties. Due to the progress in optical technologies, at the beginning of 2000's, federated

network of lidars were established (MPLNET, Welton et al., 2002, Campbell et al., 2002, Lolli et al., 2013; EARLINET, Pappalardo et al., 2014). Those instruments, due to their very high spatial and temporal resolution, are particularly well suited to retrieve vertically resolved optical and microphysical properties of aerosol and clouds. Nevertheless, different lidar techniques make different assumptions to solve the lidar equation (Eq. 1) defined as:

$$P(r) = K\frac{\beta(r)}{r^2}exp^{-2\int_0^r \alpha(r')dr'} \quad (1)$$

where *P(r)* is the received power at a range *r; K* is the so-called lidar constant, which is depending on parameters as detector quantum and optical efficiencies, telescope diameter, instrument overlap function, etc.; *β(r)* is the backscattering coefficient and *α(r)* is the extinction coefficient. It is clear that to solve the equation, which contains two unknowns at each range bin r (α and β), some major assumptions should be made. A classical method (Fernald, 1984) consists in assuming that the ratio of the two coefficients, typically indicated by S and called lidar ratio has a constant value. This assumption is pretty strong as S shows a large variability (20sr-150sr; Ackermann, 1998) depending on aerosol species, with a consequent large uncertainty associated to the retrieval of α and β. On the contrary, the combined detection of the elastic backscattered radiation and of the inelastic backscattering from the Raman roto-vibrational spectrum of nitrogen (or oxygen), using the Raman lidar technique, permits to solve directly determine the vertical profile of

Nevertheless, the Raman technique shows instability in retrieving the aerosol extinction coefficient and to reduce the random error affecting the retrieval the application of a smoothing technique is required, with a consequent descrease of the

47 effective vertical resolution of the aerosol extinction coefficient profile. In
48 conclusion, the use if different lidar techniques and different processing algorithms
49 may lead to differences in the retrieval of vertically resolved aerosol optical
50 properties, affecting both the intensity, the position and the geometry of the
51 observed aerosol nd cloud layers.
52 Though the uncertainties affecting the elastic and Raman lidar techniques are well
53 known and largely documented in literature, the impact of this difference on the
54 various end users applications has been never extensively quantified, In particular,
55 lidar profiles optical properties obtained from different techniques are more and
56 more used to assess the radiative effects of clouds and aerosols (Campbell et al.,
57 2016, Lolli et al., 2016): the differences between different type of lidar retrievals are
58 corresponding to uncertainties in determining the net radiative forcing which may
59 provide inconsistencies in studies carried out at the global scale involving different
60 lidar instrument and techniques. For this reason, it is crucial to quantitatively assess
61 the effect of different lidar techniques and data on the estimation of the radiation
62 forcing of aerosol and clouds. To reach this objective, during the short-term mission
63 at CNR in Tito Scalo, Potenza, Itay, we evaluated how much is the difference in net
64 radiative forcing calculations from the Fu-Liou-Gu radiative transfer model (FLG; Fu
65 and Liou, 1992, Fu and Liou, 1993, Gu et al., 2003, Gu et al., 2011) with respect to the
66 elastic and to the combined Raman elastic lidar techniques. This study highly
67 relevant to investigate the INTERACT-II campaign dataset in order to fully exploit
68 data following an appropriate data analysis for the different lidar techniques
69 deployed. Conclusions from this study also allows to assess impact of the lidar

retrievals on the difference in cirrus cloud radiative transfer calculations estimated using different radiative transfer models, for our case between the Corti model (simplified solution) with the more complete FLG model combination.

2. Method

2.1 Fu-Liou-Gu radiative Transfer Model

The one-dimensional Fu-Liou-Gu radiative transfer model, developed in the early 90's, recently has been adapted to retrieve the cloud and aerosol radiative forcing using as input the aerosol and cloud lidar extinction coefficient atmospheric profile measurements (Lolli et al., 2015, Tosca et al., 2015). The FLG RT model calculates the direct effect of the aerosol forcing at each altitude level inputting the aerosol optical optical depth of the layer and for the column the partial contribution to the total AOD for each aerosol species. The FLG parameterization contemplates eighteen different types of aerosols, with single scattering aerosol properties parameterized through the OPAC (Optical Properties of Aerosol and Clouds) catalog. Differently, for cloud forcing, the FLG RT model needs as input, at each altitude level of the cloud, the *IWC* and the effective drop/crystal diameter D_e. These parameters cannot be retrieved directly by lidar measurements, for this reason we use the parameterization (for cirrus clouds especially) proposed by Heymsfield et al., 2014 where D_e and *IWC* are retrieved through the atmospheric temperature and lidar extinction profiles (Lolli et al., 2015, Tosca et al., 2015). The efficacy of Heymsfield et al., 2014 is evaluated through Cloudnet radar-based retrieval of the *IWC (Illingworth et al., 2014 BAMS)*. Cloudnet processing, based on ceilometer, microwave radiometer

and Doppler radar data provides a categorization of liquid droplets, ice particles, aerosols based on different sensitivity of lidar and radar to different particle size ranges. For layers identified as ice clouds, the ice water content (with the related uncertainty) is derived from radar reflectivity factor and temperature using an empirical formula derived using aircraft data (Hogan et al.,2005).

2.2 Lidar

Lidar instruments are high-resolution optical devices capable to retrieve optical and microphysical characteristics of aerosols, clouds and precipitations (Lolli et al., 2013). As discussed in the introduction, depending on the adopted lidar technique, i.e. elastic, Raman etc., the data-handling requires a number of assumptions that may influence the determination of the net forcing. Since the lidar equation has two unknowns (Lolli et al., 2013), elastic single-wavelength lidars need a strong assumption to retrieve the extinction coefficient, input of the FLG model: the values of the lidar ratio (S), defined as the ratio between the aerosol extinction and backscattering coefficients. For aerosols, S shows a large variability in the range typically within 20-120 sr (Ackermann, 1998) influencing then drastically the consequent retrieved extinction profile. On the contrary, Raman technique has been successfully used for measurement of aerosol and cloud extinction, being the retrieval independent of any assumption Raman signals, however, is characterized by a much lower signal-to-noise ratio respect to the elastic signal (Ansmann et al., 1992): therefore large integration time are required along with the application of smoothing filters that reduce the effective vertical resolution of the retrieved

profiles (Iarlori et al., 2015 AMT) but also the relative error. In this work, a limit has been fixed on the maximum relative error of both the synthetic and real lidar profiles to values within 30-40%.

2.3 Analysis

The quantitative information on different lidar techniques and data processing was carried out on real lidar data, taken with MUSA (Multi-wavelength System for Aerosols) Lidar, deployed at CNR-IMAA Atmospheric Observatory (CIAO) in Potenza, Italy. This multi-wavelength Raman lidar instrument is a mobile reference EARLIENT system (Pappalardo et al., 2014, AMT) with a multi-year database of available measurements.

The analysis has been carried out as follows:

1) On a real aerosol dust outbreak. The used wavelength to retrieve the extinction profile is in the UV (355nm). The extinction profile is retrieved both with the Raman technique and with the elastic channel using an iterative algorithm (Di Girolamo et al., 1998) with the S value assigned from the analysis of climatological data (in this analysis S=45 sr). For the elastic channel retrievals, the signals have been smoothed using the Savitzky-Golay filter (Iarlori et al., 2015 AMT) with a resolution of 60 and 380m respectively.
2) For a real lidar measurement of cirrus clouds. Again the impact of the retrieval on cirrus cloud extinction is assessed for Raman technique and smoothing filter using different resolution windows.

The thermodynamic profile of the atmosphere, needed to calculate the net radiative forcing, is calculated with the standard thermodynamics profile (USS976) mid-latitude model. Emissivity and albedo values are taken from MODIS BRDF/Albedo algorithm product (Strahler et al., 1999), with a spatial resolution of 0.1 degrees averaged over 16 days temporal window. As each measured cloud and aerosol profile comes with the relative uncertainty, the sensitivity of the FLG RT model to the input parameters is evaluated applying a Monte Carlo technique. Each extinction profile is replicated 30 times (i.e. a number statistically meaningful) running the Monte Carlo code on the original profile uncertainty. Likewise for each replicated extinction profile, the Monte Carlo technique gives a value of surface albedo and profile temperature, based on their respective uncertainties. The radiative forcing of each profile is then represented with a histogram. The smoothing uncertainty is then quantified from the mean and the standard deviation of the net forcing for the profile set.

3. First results

The analyzed dust event is chosen from measurements taken on 3 July 2014 at CIAO. Figure 1 shows the lidar aerosol extinction profiles at 355 nm obtained using the Raman technique with an effective resolution of 360 m and the same profile obtained using the elastic lidar technique at two different resolutions (60m and 360m) using a fixed S value if 45 sr, determined by climatological measurements are represented in Figure 1. It can be immediately recognized that Raman extinction coefficient is much more noisy with respect to the same profiles obtained with the

161 iterative method. Nevertheless, all the profiles, obtained with a temporal resolution
162 of 60 minutes, are cut at about 5.5 Km, as after this altitude level any significant
163 aerosol feature is missing, and then the signals are prone to represent noise. Figure
164 3 shows the difference between the estimation of the net forcing suing the two
165 considered lidar technique and data processing: it appears as the most important
166 contribution to this different in FLG calculations for the aerosol are related to the
167 adopted lidar technique (red arrow in Fig. 3, upper and bottom panels) and not in
168 effective vertical resolution determined by the smoothing (blue arrow in Fig. 3,
169 upper and bottom panels), . This characteristic is invariant both at TOA and SFC and
170 it is mainly the result of the assumption of a fixed lidar to calculated the aerosol
171 extinction profile using the elastic lidar technique. In the considered Saharan dust
172 case, the net radiative forcing determined with the two different lidar techniques
173 differ of about 0.7 W/m^2 at SFC and of 1.0 W/m^2 at TOA: this quantity is much larger
174 than the uncertainty average estimated direct effect by IPCC (mean 0.5 W/m^2, range
175 -0.9 to -0.1 with. The contribution due to the smoothing is negligible. This show how
176 the mixing of different lidar techniques in a specific study or in the routine
177 operation of an aerosol network at regional or global scale must take into account of
178 the uncertainties related to the assumptions which are behind the retrieval of the
179 optical properties. This is important not only to provide a complete assessment of
180 the total uncertainty budget for each lidar product but to enable a physically
181 consistent use of the lidar data in the estimation of the radiative forcing and, likely,
182 for many other user-oriented applications based on lidar data. Figure 4 depicts the
183 results performing the same analysis but for a cirrus cloud on 16 February 2014

(signals in Fig. 2). The obtained cloud extinction profiles with the different lidar techniques and data processing are averaged over of 60 minutes. Here we have a completely different situation compared to aerosol: for clouds, the differences between Raman and elastic lidar techniques (red arrow in Fig. 4, upper and bottom panels) are much smaller that the differences due to the effective vertical resolution of the aerosol extinction coefficient profile (blue arrow in Fig. 4, upper and bottom panels). This is related to the typical much stronger and faster increase of the aerosol extinction for a clouds than for aerosol. In the considered cirrus cloud case, the net radiative forcing determined with the two different lidar techniques differs about of 0.5 W/m^2 at SFC and of -2 W/m^2 at TOA, while the effect of smoothing on a window of 420 m provides and additional uncertainty of more than 2 W/m^2 at the SFC and of about -11 W/m^2 at TOA. This implies the need for high resolution lidar measurements of the cirrus clouds to provide an accurate estimation of their forcing.

4. Future perspectives

We used the adapted Fu-Liou-Gu radiative transfer model as proxy to evaluate the discrepancies in aerosol optical properties retrieval using different lidar techniques and data processing/smoothing. The differences are quantified from Fu-Liou-Gu (FLG) net radiative forcing calculations at surface (SFC) and top-of–the-atmosphere (TOA). The results put in evidence that there is not variability for TOA and SFC, while for dust event the data processing/smoothing it is not very influent, but instead the lidar technique it is important. The opposite is true for the cirrus cloud,

where the data processing/smoothing play a fundamental role. A possible explanation of this behavior is due to the different optical depth of the clouds with respect to the aerosol dust layer. Summarizing, as the optical depth in both cases it is the driving parameter, at coarse resolution (cloud) the smoothing is producing changes in the extinction profile that translates in creation/suppression of ice crystals that have a heavy influence on forcing. While at fine resolution, as in the case of dust event, the smoothing is just producing fluctuations that don't influence the total forcing. In this case the lidar technique is picking up, as the wrong S value can amplify or suppress the aerosol peak that translates into a higher/lower forcing.

References

Ackermann J., 1998: The Extinction-to-Backscatter Ratio of Tropospheric Aerosol: A Numerical Study. *J. Atmos. Oceanic Technol.*, **15**, 1043–1050.

Ansmann, A., M. Riebesell, and C. Weitkamp, 1990: Measurement of atmospheric aerosol extinction profiles with a Raman lidar. *Opt. Lett*, **15,** 746–748

Bösenberg, J and R Hoff ,2008 GAW Aerosol Lidar Observation Network (GALION), WMO GAW Report in press (WMO, Geneva, Switzerland)

Campbell et al., 2002 "Aerosol Lidar Observation at Atmospheric Radiation Measurement Program Sites: Instrument and Data Processing," J. Atmos. Oceanic Technol., 19, 431-442

Fu Q, Liou KN, 1992: On the correlated k-distribution method for radiative transfer in nonhomogeneous atmospheres. J. Atmos. Sci. 49:2139 2156.

Fu Q, Liou KN, 1993: Parametrization of the radiative properties of cirrus clouds. J. Atmos. Sci. 50:2008-2025.

Gu Y, Farrara J, Liou KN, Mechoso CR, 2003: Parametrization of cloud-radiativeprocesses in the UCLA general circulation model. J. Climate 16:3357-3370.

Gu Y, Liou KN, Ou SC, Fovell R, 2011: Cirrus cloud simulations using WRF with improved radiation parametrization and increased vertical resolution. J. Geophys. Res.116:D06119.

Heymsfield, A., D. Winker, M. Avery, M. Vaughan, G. Diskin, M. Deng, V. Mitev, and R. Matthey, 2014: Relationships between ice water content and volume extinction coefficient from in situ observations for temperatures from 0° to

239 −86°C: Implications for spaceborne lidar retrievals. *J. Appl. Meteor. Climatol*.,
240 53, 479–505
241 IPCC, 2012: Managing the Risks of Extreme Events and Disasters to Advance Climate
242 Change Adaptation. A Special Report of Working Groups I and II of the
243 Intergovernmental Panel on Climate Change [Field, C.B., V. Barros, T.F.
244 Stocker, D. Qin, D.J. Dokken, K.L. Ebi, M.D. Mastrandrea, K.J. Mach, G.-K.
245 Plattner, S.K. Allen, M. Tignor, and P.M. Midgley (eds.)]. Cambridge University
246 Press, Cambridge, UK, and New York, NY, USA, 582 pp.
247 IPCC, 2014: *Climate Change 2014: Impacts, Adaptation, and Vulnerability. Part A:*
248 *Global and Sectoral Aspects. Contribution of Working Group II to the Fifth*
249 *Assessment Report of the Intergovernmental Panel on Climate Change* [Field,
250 C.B., V.R. Barros, D.J. Dokken, K.J. Mach, M.D. Mastrandrea, T.E. Bilir, M.
251 Chatterjee, K.L. Ebi, Y.O. Estrada, R.C. Genova, B. Girma, E.S. Kissel, A.N. Levy,
252 S. MacCracken, P.R. Mastrandrea, and L.L. White (eds.)]. Cambridge
253 University Press, Cambridge, United Kingdom and New York, NY, USA, 1132
254 pp.
255 Khor W. Y, Matjafri M. Z., Lim H.; Hee W. S ; Lolli S., 2015: One-year monitoring of
256 the atmosphere over Penang Island using a ground-based lidar Proc. SPIE
257 9645, Lidar Technologies, Techniques, and Measurements for Atmospheric
258 Remote Sensing XI, 96450M (October 20, 2015); doi:10.1117/12.2195440.
259 Lolli S. et al, 2013, "Evaluating light rain drop size estimates from multiwavelength
260 micropulse lidar network profiling.,"*J. Atmos. Oceanic Technol.*, **30**, 2798–
261 2807.

Lolli S. ; E. J. Welton ; A. Benedetti ; L. Jones ; M. Suttie ; S-H. Wang. 2014." MPLNET lidar data assimilation in the ECMWF MACC-II Aerosol system: evaluation of model performances at NCU lidar station." Proc. SPIE 9246, Lidar Technologies, Techniques, and Measurements for Atmospheric Remote Sensing X, 92460I (October 20, 2014); doi:10.1117/12.2068201

Pappalardo et al. ACP or AMT 2015.

Strahler, A. H., C. B. Schaaf, J.-P. Muller, W. Warmer, M. J. Barnsley, R. d'Entremont, B. Hu, P. Lewis, X. Li, and E. V. Ruiz de Lope, 1999: MODIS BRDF/albedo product: Algorithm theoretical basis document. NASA EOS-MODIS Doc. ATBD-MOD-09, version 5.0

Welton E. J., et al., 2002: "Measurements of aerosol vertical profiles and optical properties during INDOEX 1999 using micropulse lidars," *J. Geophys. Res.*, 107, 8019

Figures

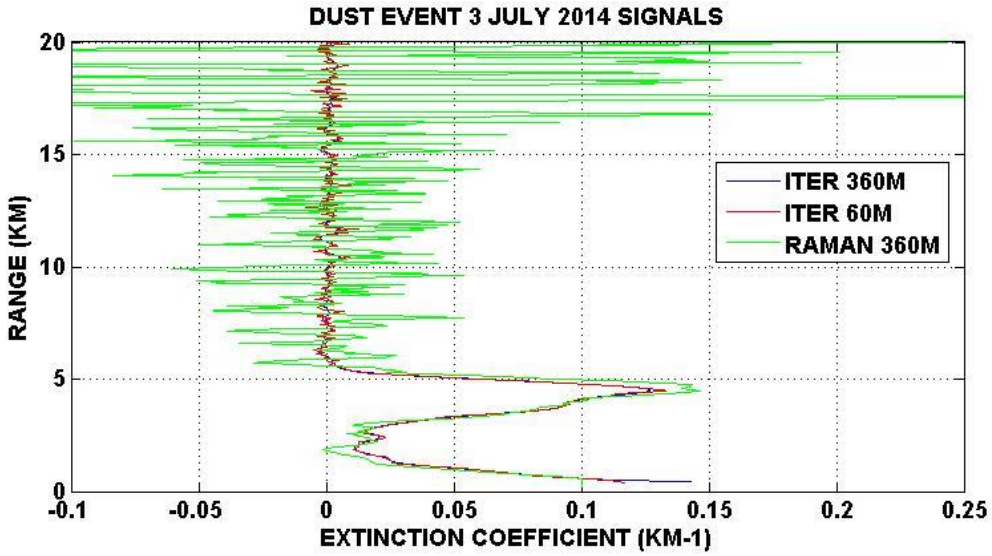

Figure 1 Lidar extinction profiles at 355nm from Raman and elastic channel respectively for dust outbreak on 3 July 2014. The iterative method at the two different resolutions (60m and 360m) used a fixed S value, determined by climatological measurements

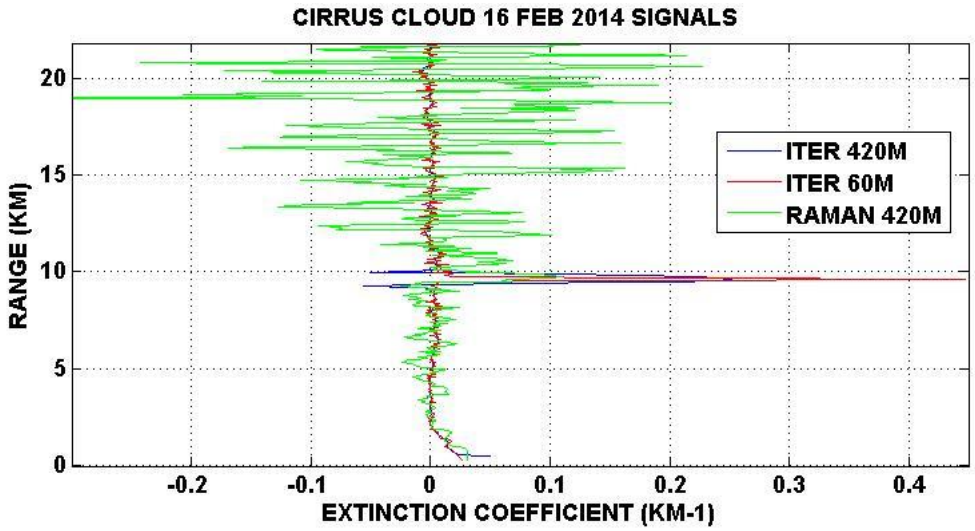

Figure 2: Lidar extinction profiles at 355nm from Raman and elastic channel respectively a cirrus cloud on 16 Febraury 2014. The iterative method at the two different resolutions (60m and 420m) used a fixed S value, determined by climatological measurements

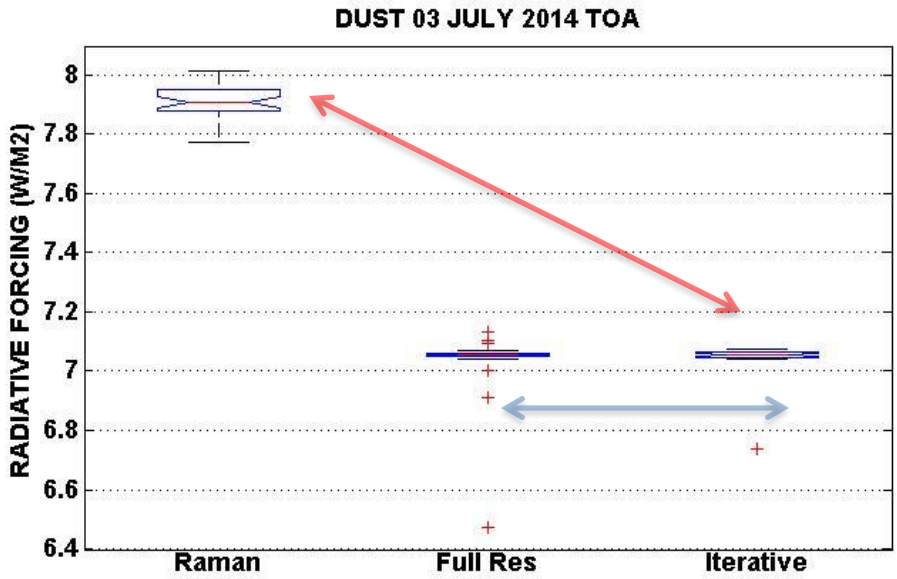

287

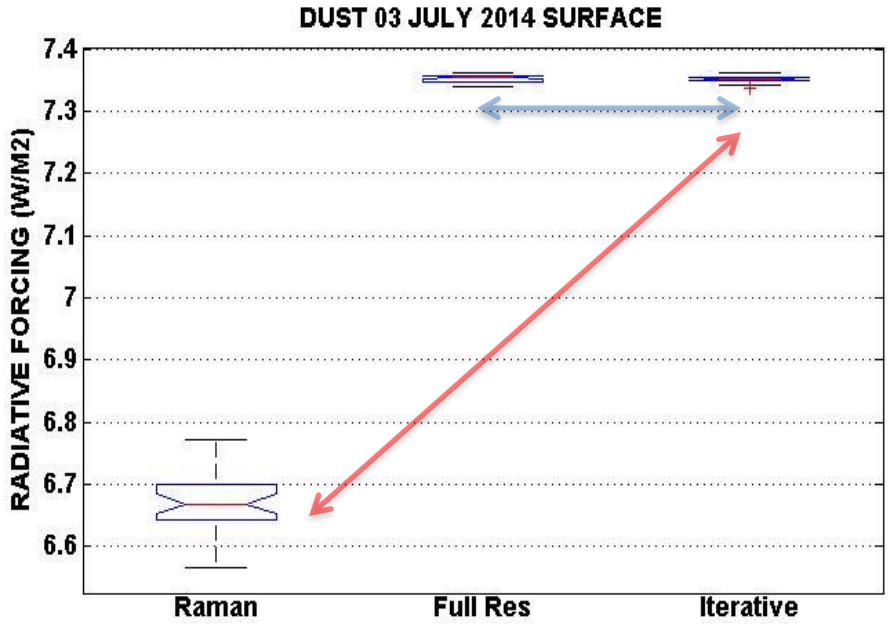

288

289 Figure 3 Dust event of 03 July 2014. The net radiative forcing is calculated at TOA and SFC
290 respectively. As it is clearly visible, the larger discrepancy in forcing is related mostly to the lidar
291 technique (red arrow), not on data processing (blue arrow).

292

293

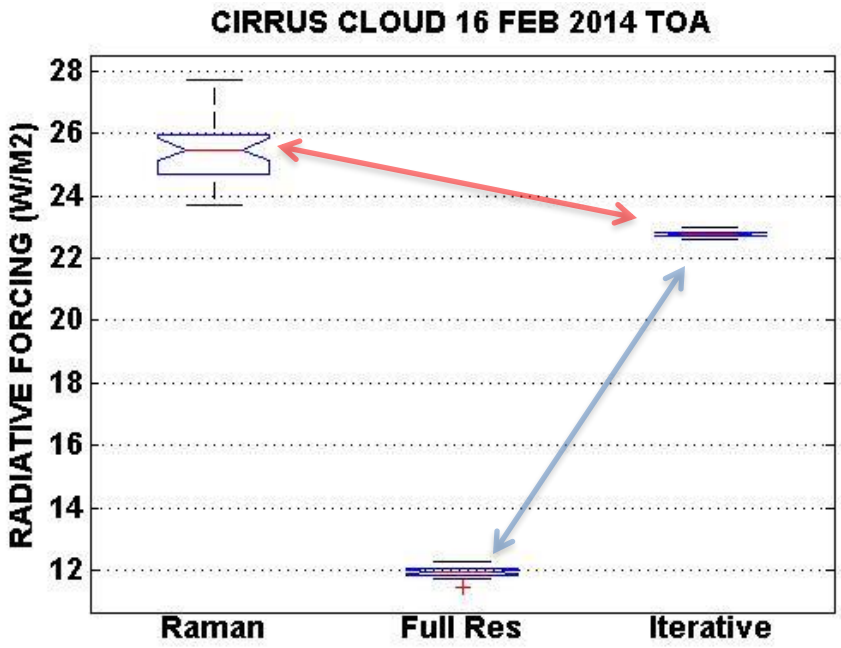

294

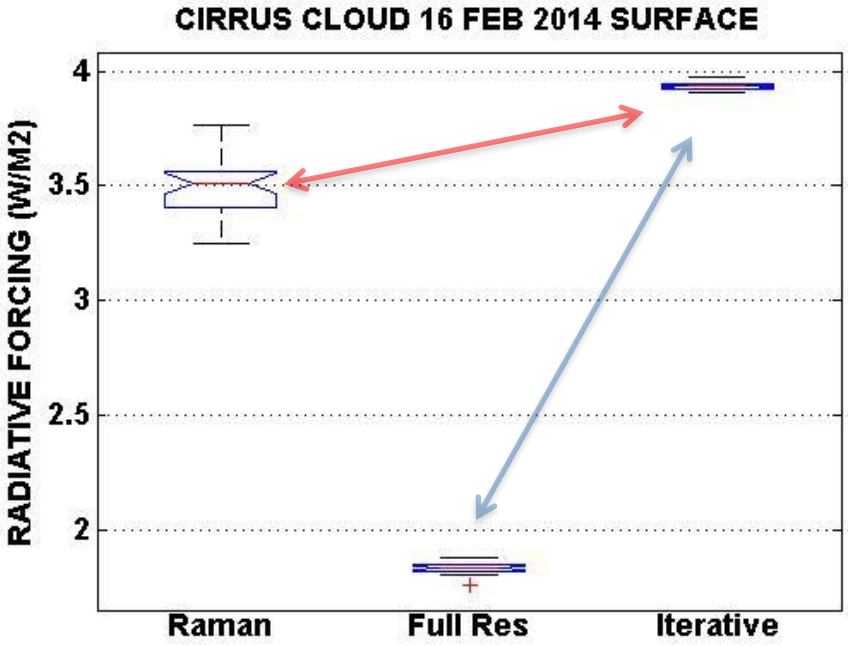

295

296 Figure 4 Cirrus Cloud of 16 Feb 2014. The net radiative forcing is calculated at TOA and SFC
297 respectively. As it is clearly visible, the larger discrepancy in forcing is related mostly to the data
298 processing (blue arrow), not on lidar technique (red arrow).

299